Results from the 50-micron Pitch Diamond Tracker in the RD-42 May '95 Beam Test at CERN

John Conway
Rutgers University

June 27, 1995

Abstract

Data from the May '95 beam test at CERN yield results on the spatial resolution, signal-to-noise, and efficiency of a 50-micron-pitch CVD diamond tracking detector. Full details of the test beam telescope, alignment, and algorithms are given. Though a signal to noise ratio of 30 is obtained, the measured position resolution, 12.8 μm, is only slightly better than digital resolution, for reasons not yet understood.

1 Overview

In May of 1995 several CVD diamond microstrip tracking detectors were tested in a 100 GeV pion beam at CERN. Among these detectors was the first such device plated with microstrips with 50-micron-pitch strips. Since this represents the typical strip pitch of silicon microstrip detectors currently in use, one would like to determine whether the signal to noise and position resolution of a diamond detector can approach that of silicon.

The test utilized a set of eight silicon microstrip detectors, with the diamond detectors in the middle. The silicon detectors define the trajectory of a charged particle through the diamond detectors under study, and allow rejection of events with more than one charged particle. Knowing the precise position of each charged particle, one can examine the position resolution and signal to noise ratio of the diamond in an unbiased way. Hundreds of thousands of events were recorded with varying conditions of detector high voltage and levels of exposure to ionizing radiation. The main measurements addressed in this analysis of the data

- the best obtainable position resolution for the diamond detector,
- the signal to noise ratio and efficiency in this detector, and
- the effect of exposure to radiation ("pumping") on the signal to noise and resolution.

2 Alignment and Track Fitting

The spatial arrangement of the test telescope lends itself naturally to a coordinate system in which each detector plane measures a coordinate generically referred to as u_i for each plane

i located at z_i along the beam axis. To fully define the coordinate system one can use as reference the "0th" strip on two upstream and two downstream planes, each pair measuring roughly orthogonal directions.

There were eight silicon detector planes in the test beam, used to define the position of pions passing through the diamond detectors under study. Silicon planes 1, 3, 5, and 7 nominally measured the x coordinate, and planes 2, 4, 6, and 8 measured y. We use the planes 1, 2, 5, and 6 to define the coordinate system. Thus the z axis is that line passing through the zeroth strip on each of these planes. The x axis points perpendicularly to the z axis, and is perpendicular to the strips on detectors 1 and 5, and similarly for the y detectors 3 and 7. Note that this leaves the possibility that a) the x and y axes are not perfectly orthogonal, and b) there may be some "torsion" in the coordinate system in going from upstream to downstream. As shown below, however, these effects are negligibly small.

We wish to measure the positions of the other four silicon planes (and later the diamond planes) relative to the reference planes. For each plane i one must determine in principle one offset u_{0i} in the direction perpendicular to the strips, an angle of rotation θ_i about the z axis, an angle of rotation ψ_i about the u_i axis, and and angle ϕ about the zeroth strip axis. In practice, however, the effect of the angles ψ and ϕ is negligibly small, and they are ignored. The relationship between u and the x an y axes is straightforward:

$$u_i = +x_i \cos\theta_i + y_i \sin\theta_i \quad . \tag{1}$$

We define analogously a coordinate v in each plane which lies along the strips in that plane:

$$v_i = -x_i \sin\theta_i + y_i \cos\theta_i \quad . \tag{2}$$

To determine the alignment of the non-reference silicon planes we use a large ensemble of tracks fit with the reference planes. Each track can be specified by four parameters, a_0, a_1, b_0, and b_1 where

$$x(z) = a_0 + a_1 z \tag{3}$$
$$y(z) = b_0 + b_1 z \tag{4}$$

give the projections in the $x - z$ and $y - z$ planes. The fit track minimizes χ^2 defined as

$$\chi^2 = \sum_{i=1}^{n_{ref}} \frac{(u_i^{hit} - u_i^{track})^2}{\sigma_i^2} \tag{5}$$

The track parameters result from setting the derivative of χ with respect to each parameter to zero:

$$\begin{pmatrix} a_0 \\ a_1 \\ b_0 \\ b_1 \end{pmatrix} = \sum_i \begin{pmatrix} \frac{\cos^2\theta_i}{\sigma_i^2} & \frac{z_i\cos^2\theta_i}{\sigma_i^2} & \frac{\sin\theta_i\cos\theta_i}{\sigma_i^2} & \frac{z_i\sin\theta_i\cos\theta_i}{\sigma_i^2} \\ \frac{z_i\cos^2\theta_i}{\sigma_i^2} & \frac{z_i^2\cos^2\theta_i}{\sigma_i^2} & \frac{z_i\sin\theta_i\cos\theta_i}{\sigma_i^2} & \frac{z_i^2\sin\theta_i\cos\theta_i}{\sigma_i^2} \\ \frac{\sin\theta_i\cos\theta_i}{\sigma_i^2} & \frac{z_i\sin\theta_i\cos\theta_i}{\sigma_i^2} & \frac{\sin^2\theta_i}{\sigma_i^2} & \frac{z_i\sin^2\theta_i}{\sigma_i^2} \\ \frac{z_i\sin\theta_i\cos\theta_i}{\sigma_i^2} & \frac{z_i^2\sin\theta_i\cos\theta_i}{\sigma_i^2} & \frac{z_i\sin^2\theta_i}{\sigma_i^2} & \frac{z_i^2\sin^2\theta_i}{\sigma_i^2} \end{pmatrix} \sum_i \begin{pmatrix} \frac{u_i\cos\theta_i}{\sigma_i^2} \\ \frac{u_i z_i\cos\theta_i}{\sigma_i^2} \\ \frac{u_i\sin\theta_i}{\sigma_i^2} \\ \frac{u_i z_i\cos\theta_i}{\sigma_i^2} \end{pmatrix} \tag{6}$$

3 Cluster Finding and Hit Position

In order to determine u_i^{hit} in each plane a hit cluster finding and position algorithm must be employed. The algorithm here operates by iteratively searching in each plane for the strip with the maximum pulse height, marking that strip and its two neighbors as "used," and looping until no unused strips with pulse height above some threshold remain. If the strip with maximum pulse height lies next to a (used) strip with larger pulse height, or within two strips of a previous maximum, that strip is not considered part of a hit cluster. This algorithm results in a list of hit clusters for each plane.

This analysis used only those events in which there was only one hit cluster in each silicon plane. A threshold of 10 ADC counts was used to suppress noise hits. (The noise in the silicon planes was roughly 1.5 ADC counts rms.)

The hit position u_i was determined from the relation

$$u_i = u_{0i} + d_i s_i \tag{7}$$

where d_i represents the strip pitch (50 μm for silicon planes), and s_i represents the position of the hit cluster in strip units. This value was simply the pulse-height-weighted average of the positions of the central strip and the adjacent strip with highest pulse height. Various algorithms were studied, with this giving near-optimal good position resolution. The efficacy of an "eta deconvolution" algorithm is discussed below.

4 Alignment Results

Using a large ensemble of tracks fit with the four reference silicon planes, one can determine the offset u_{0i} and rotation θ_i from the distribution of the residuals Δu_i, defined as

$$\Delta u_i = u_i^{hit} - u_i^{track} \quad . \tag{8}$$

The two parameters can be found by from the two-dimensional distribution of Δu and v in each plane. One makes a linear best fit to the distribution, which can be parametrized as

$$\Delta u_i = \Delta u_{0i} - v_i \tan(\Delta\theta_i) \quad , \tag{9}$$

from which the adjustments Δu_{0i} and $\Delta\theta_i$ can be extracted.

Figures 1 and 2 show the mean residuals in the silicon versus u and v in each plane for the alignment of run 117. The fact that the data points do not deviate from $\Delta u = 0$ on average indicates that the final offset u_{0i} needs no adjustment. Likewise the lack of any dependence of the mean residual on v indicates a correct rotation angle θ_i in that plane. However the plots for Y3 and Y4 show a small slope in the plot of mean residual versus u. Such an effect could be due either to a slight deviation in average strip pitch from the nominal 50 μm, or from a small rotation angle (approximately 1.4°) about the strip direction in one of the two detectors. In either case the effect leads to negligible systematic errors on the extrapolation of the track into the diamond planes and no further alignment correction is made.

5 Spatial Resolution

Of the various runs made during the test and subsequently, run 117 for example should in principle exhibit the best signal-to-noise and position resolution. In this run the 50-micron diamond (NDF_005_B, henceforth denoted as "B") was operated at 300 V after being exposed to radiation for 48 hours. The notation "B**" denotes the fact that the detector was exposed for two 24-hour periods.

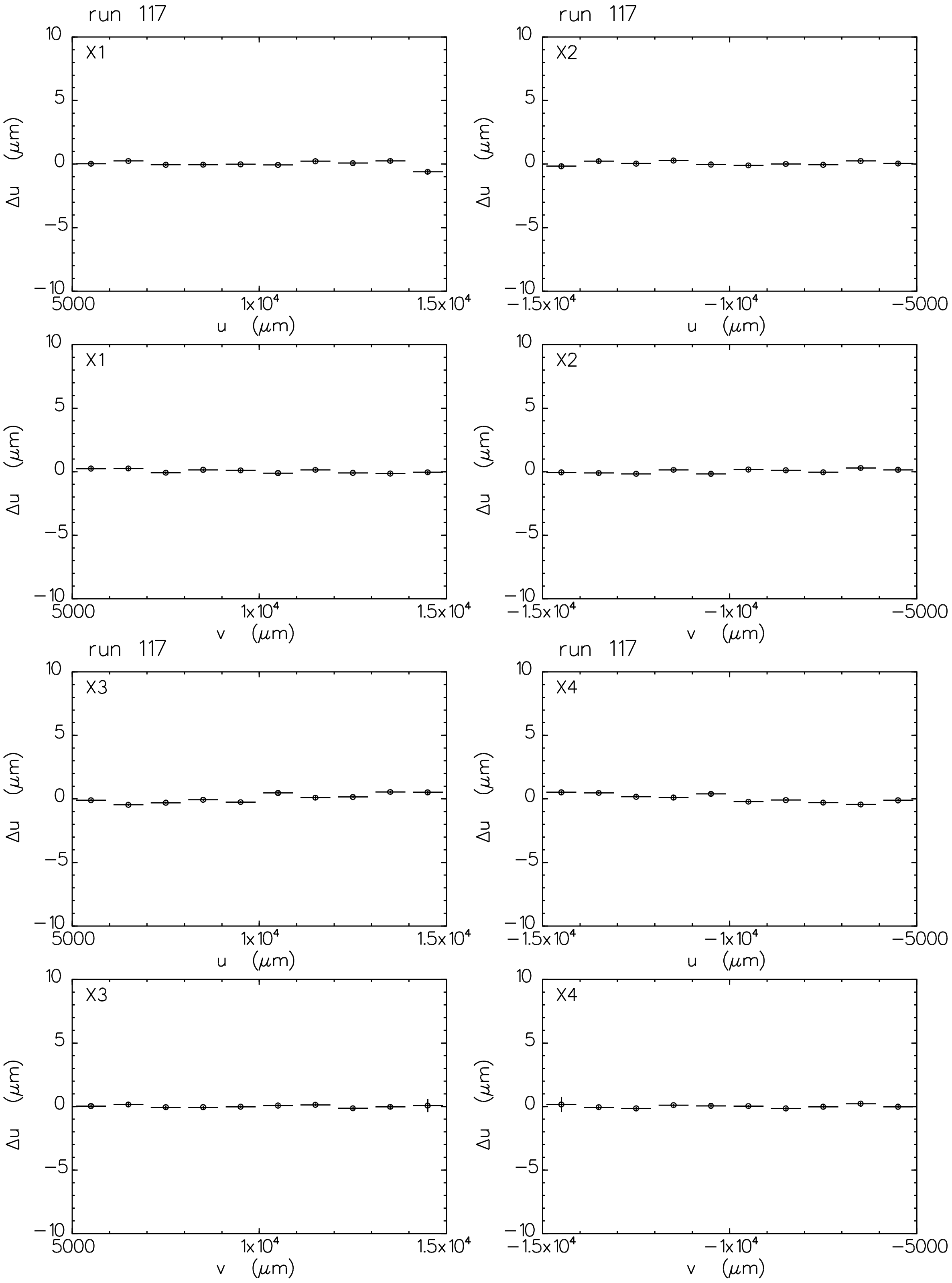

Figure 1: Mean of track residuals in each of the x silicon planes as a function of u (perpendicular to the strip direction) and v (along the strip direction) in each plane.

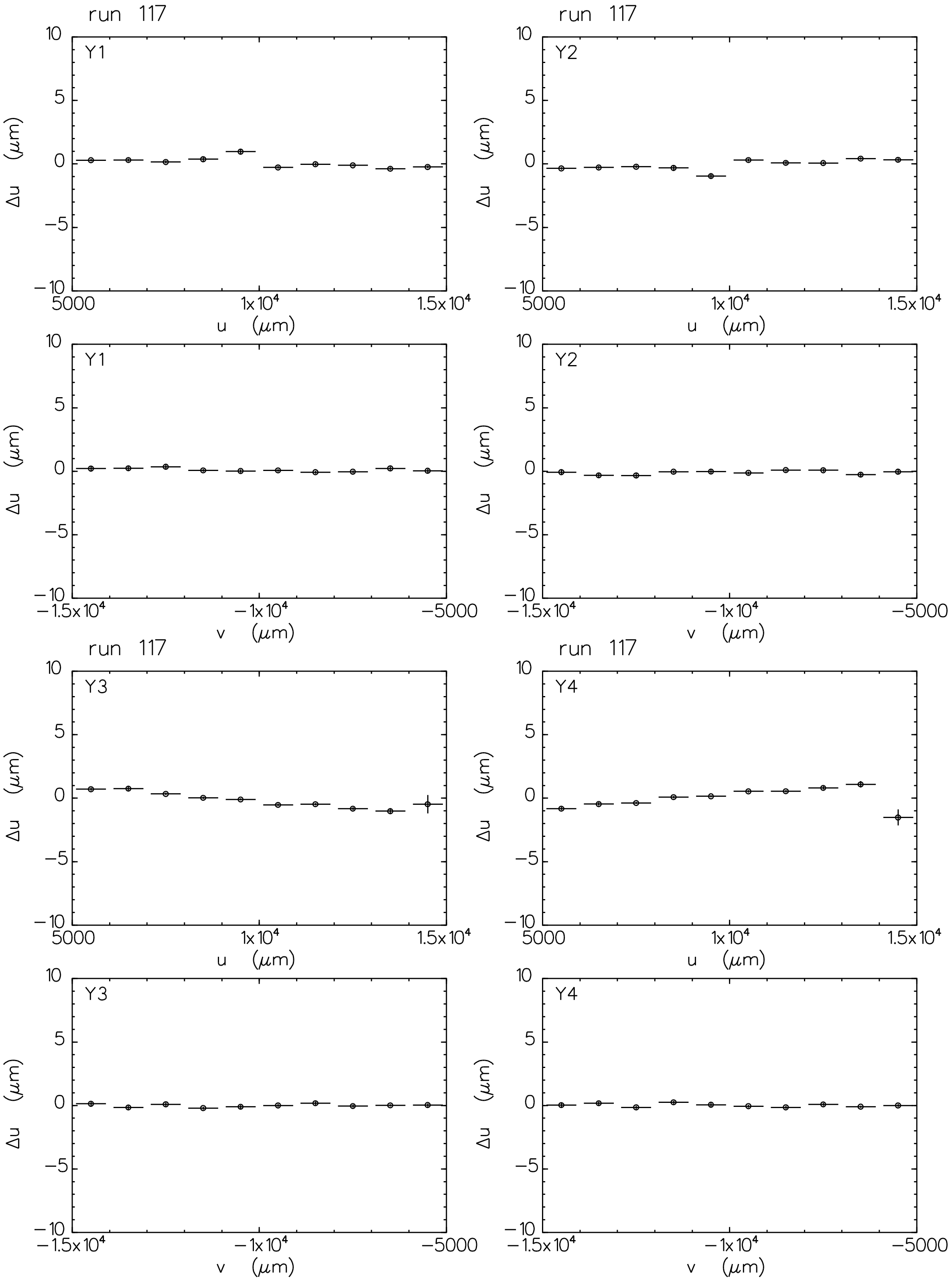

Figure 2: Mean of track residuals in each of the y silicon planes as a function of u (perpendicular to the strip direction) and v (along the strip direction) in each plane.

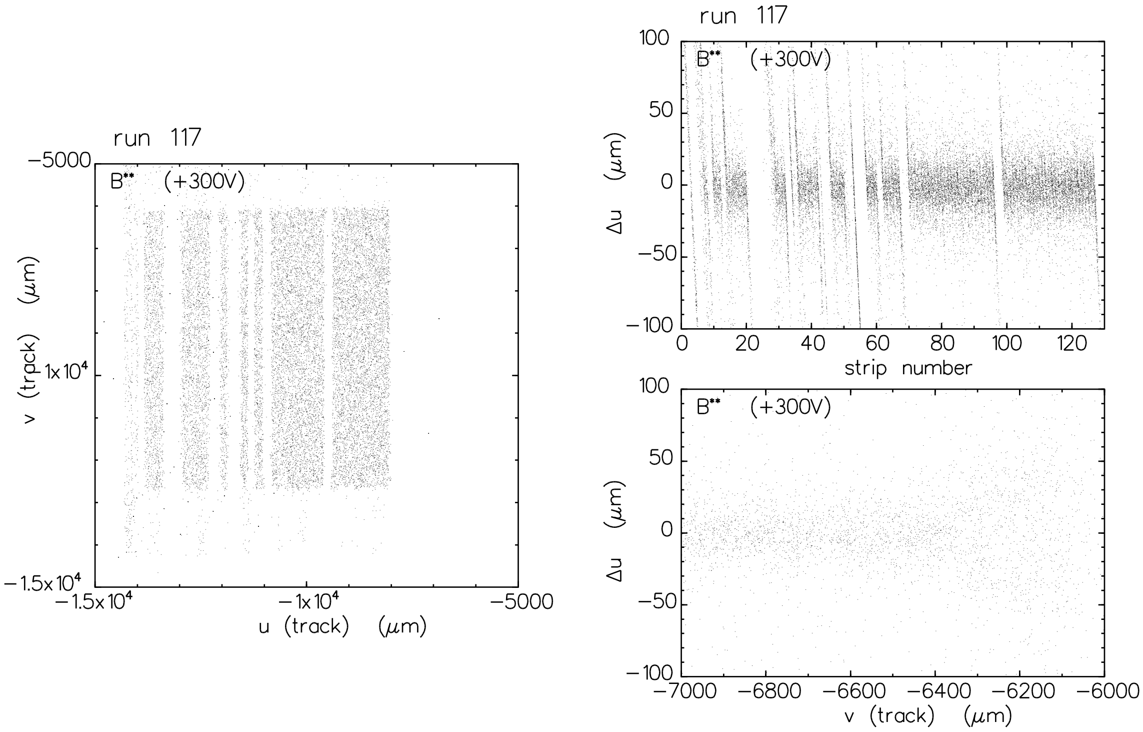

Figure 3: Left: Extrapolated track position in the 50-micron diamond plane in run 117, for tracks giving a residual of less than 100 μm. The two swaths on the right edge are the eventual fiducial region in the diamond. Right: Hit residuals as a function of strip number and position along the strip near the end of the strips.

By a procedure identical to that of the silicon planes one can align the diamond plane. Before this can be done successfully, however, it is necessary to restrict attention to a fiducial region of the detector where the electronics performed optimally. Figure 3 shows the location of the track extrapolation in the $u - v$ coordinates of the diamond plane for those tracks giving rise to a diamond hit within 100 μm of the track in u. (Clearly a rough alignment with no fiducial cuts must be made first!) This plot on the left shows two large swaths near u=-10000 μm well away from dead regions. The plot on the right shows the hit residuals as a function of the track strip position and as s a function of v, near the end of the strips. The width of the residual distributions widens considerably near the end of the strips, presumably due to field distortions. The fiducial region is then defined by the track extrapolating to the range -12000 μm $< v <$ -6500 μm, and to the strip number ranges 71-99 and 101-125. All subsequent results are only measured in this fiducial region.

Figure 4 shows the mean residual as a function of v. There is perhaps a small shift of less than a micron in the offset, and no evidence of any remaining angular shift. A gaussian fit to the distribution of Δu for the diamond then yields its position resolution, which is 12.8 μm. Figure 5 shows this distribution and fit. For the same events one can measure a signal-to-noise ratio, albeit biased by the presence of the 10 ADC count cut in the cluster finding algorithm. (An unbiased measurement appears below.) The plots in figure 6 show the distributions of pulse height and seed strip noise in units of ADC counts. The mean pulse height of 110 divided by the average rms noise of 3.6 counts would indicate a signal-to-noise ratio of about 30:1. Conservatively using the most likely value of about 70 counts gives roughly 20:1.

Given such a large signal-to-noise ratio, why is the resolution only slightly better than the 14.4 μm digital resolution to be expected from a 50-μm-pitch device? Is there more information to be employed in determining the hit position?

In previous studies the position was determined by making a mapping of the variable η to the hit position s. Here s is defined as the fraction of a strip pitch from the center of the "left" strip to the center of the "right" strip of a pair of adjacent strips. These strips are defined as discussed above, and the variable η can be written as

$$\eta = \frac{q_R}{q_L + q_R} \tag{10}$$

where q_L and q_R are the pulse heights on the left and right strips. The distribution of s is in general flat, but that of η is not; to deconvolute one simply defines s as the fraction of the integral of the whole η distribution, from zero to the measured η.

Such a procedure can clearly improve the resolution of the silicon, but as it turns out this is not the case in diamond. This is illustrated by figure 7. The plots on the left show the correlation between the residual and the variable eta for diamond, and those on the right show the same distribution for one of the silicon planes. Note the order of magnitude difference in scales on the vertical axis; the silicon resolution is about 1.5 μm, whilst that of the diamond is about 13 μm. More importantly, however, the correlation plots illustrate that there is a "wiggle" in the silicon which the eta deconvolution algorithm would remove. No such wiggle exists in the diamond plot, and since the deconvolution can only shift a point at a given eta to higher or lower residual, there appears to be nothing to be gained in using such an algorithm for the diamond detector.

It remains to determine whether there might be any correlation with other variables. Did the alignment shift during the run? Is there a systematic dependence of the residual on pulse-height? Is the z position of the detector correct? The plots in figure 8 show no evidence of any systematic correlations of the residuals with event number or pulse height. The plot of the residual versus a quantity labeled "Δz" was made by adding a random arbitrary z offset to the diamond plane for each track. If there were an unknown shift in the z position of the plane which causes the residual distribution to be too wide, the plot would show a "pinch" at a nonzero value of Δz. No such pinch is evident, and the tilt in the plot is caused by the residual torsion in the coordinate system discussed above. The final plot in the figure shows how the residual correlates with the position s of the track. There is a slight correlation at the extremes which correspond to the strip centers. When the track passes near the center the residual can be biased by fluctuations in the side strips.

Large channel-to-channel gain variations could also contribute to the spread in the residuals. Figure 9 shows the average pulse height on the strip through which the track projects, for diamond and silicon. The channel-to-channel variation is roughly 5% in the diamond detector, much larger than that in the silicon case. However, a simple numerical model including this effect, the effect of electronic noise, and the effect of clustering predicts no more than a 2 μm rms in the residual distribution.

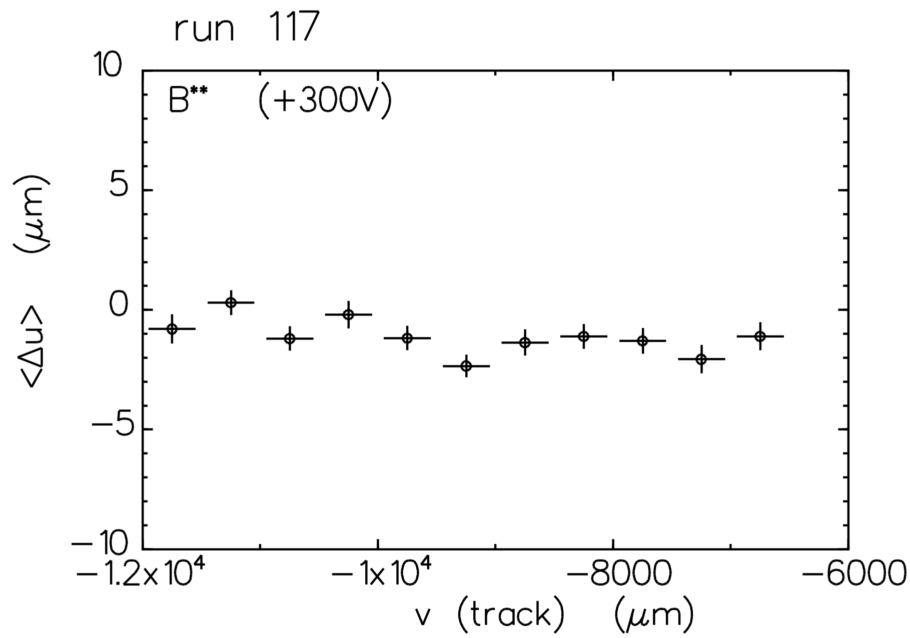

Figure 4: Mean of track residuals in each of the diamond plane as a function of v (along the strip direction) after all fiducial cuts.

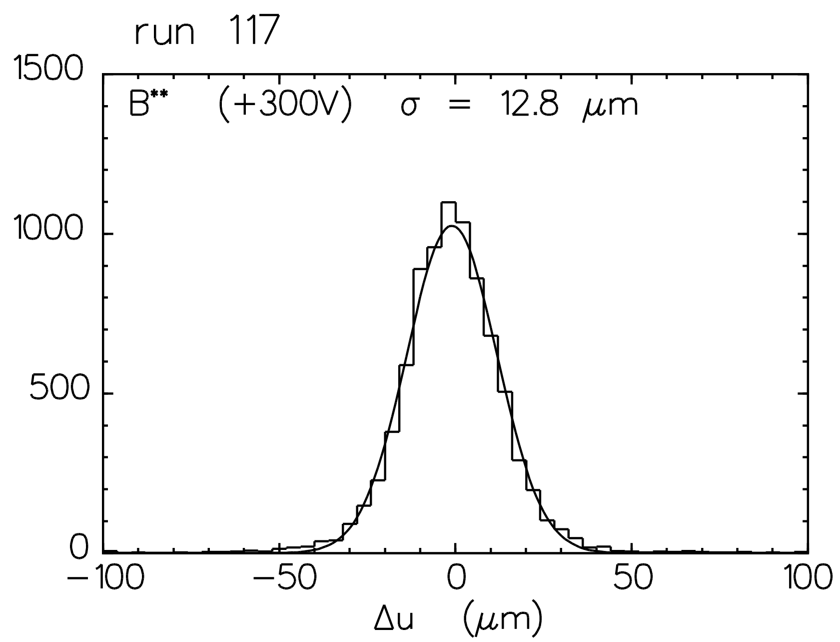

Figure 5: Distribution of track hit residuals in the 50-micron diamond after all fiducial cuts.

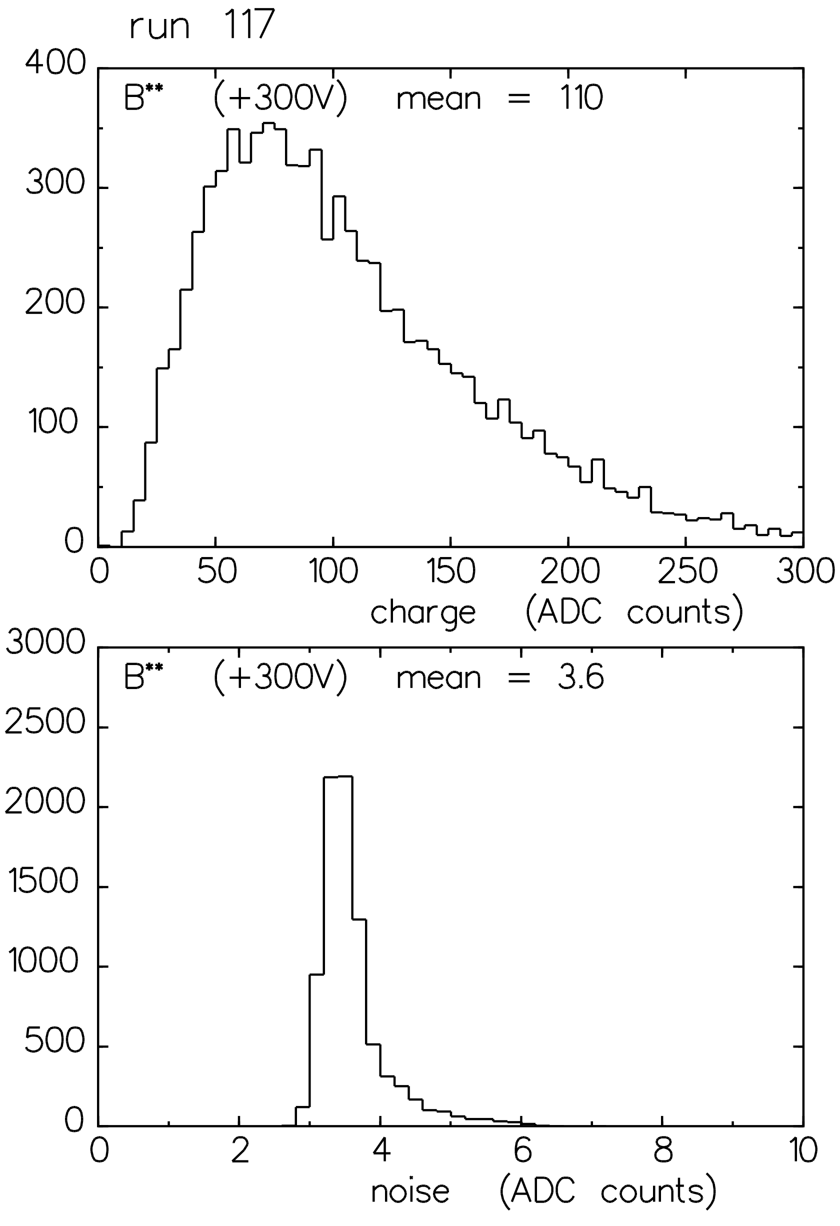

Figure 6: Pulse height distribution (above) and noise (below) in the diamond detector.

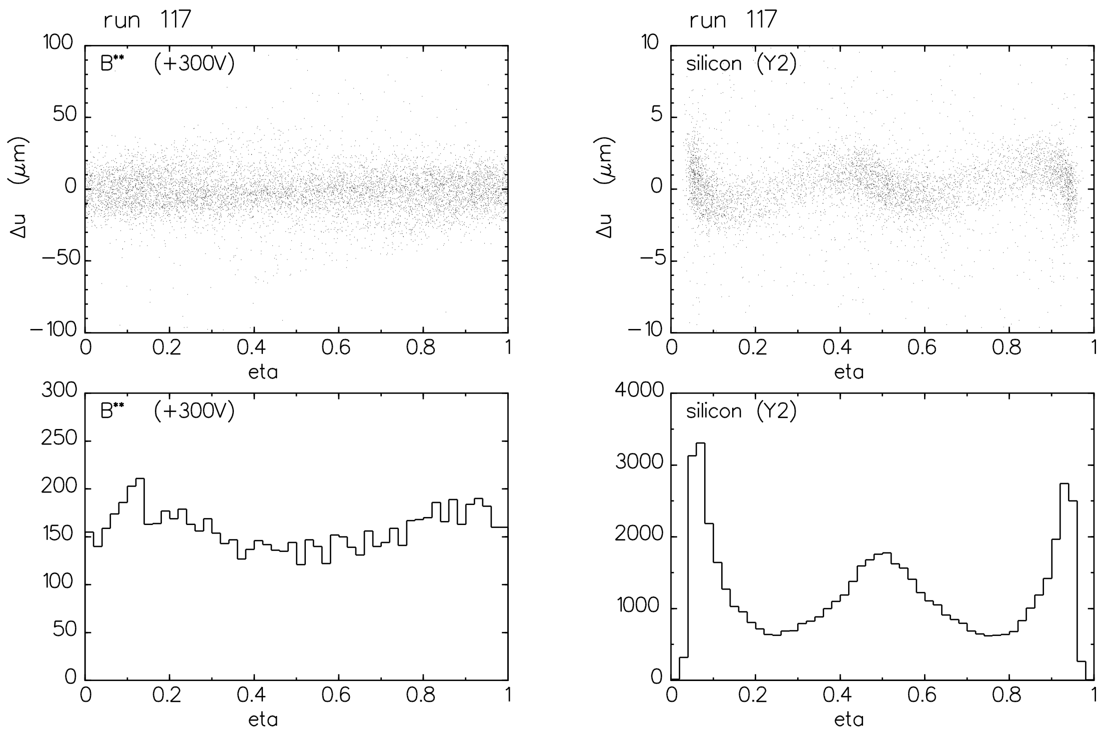

Figure 7: Track residuals in versus eta in (left) the diamond plane and (right) a typical silicon plane. The eta projections appear in the lower plots. Note the difference in vertical scales in the upper plots.

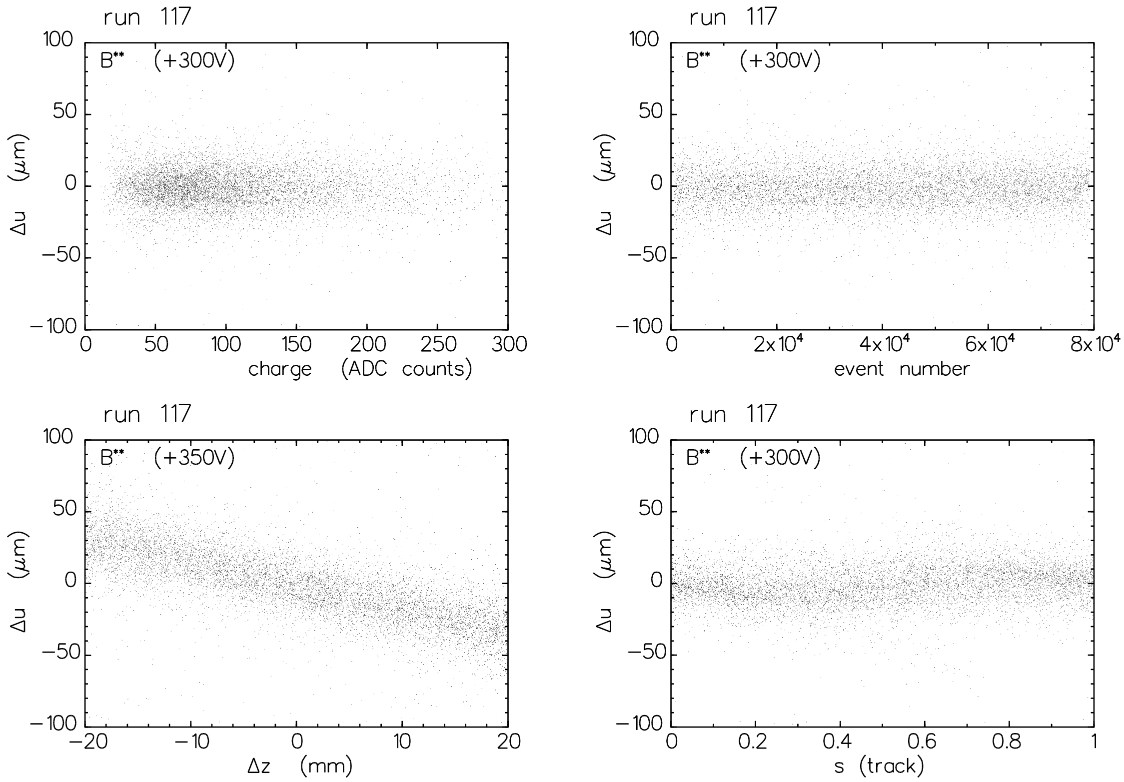

Figure 8: Track residuals in versus pulse height (upper left), versus event number (upper right), versus an arbitrary random shift in the assumed z position of the diamond plane (lower left), and versus s, the fraction of the strip pitch between the center of the left and right strips where the track extrapolates (lower right).

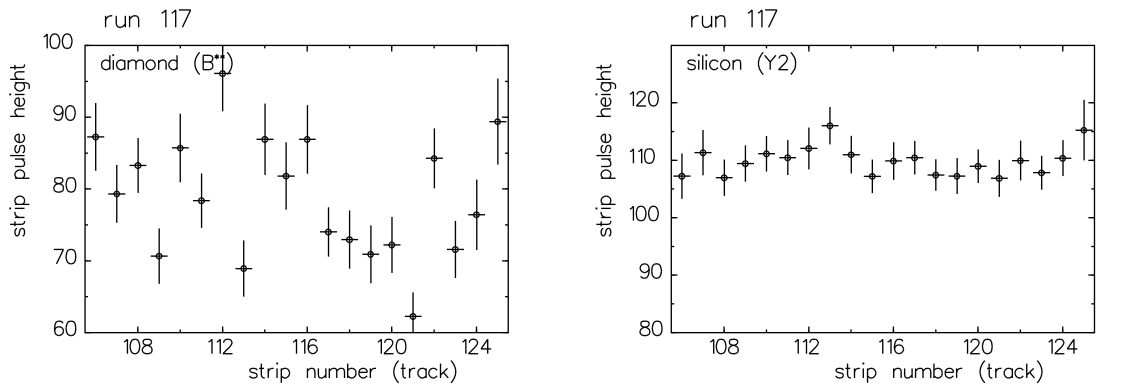

Figure 9: Average pulse height on the strip through which the track projects, comparing diamond (left) and silicon (right).

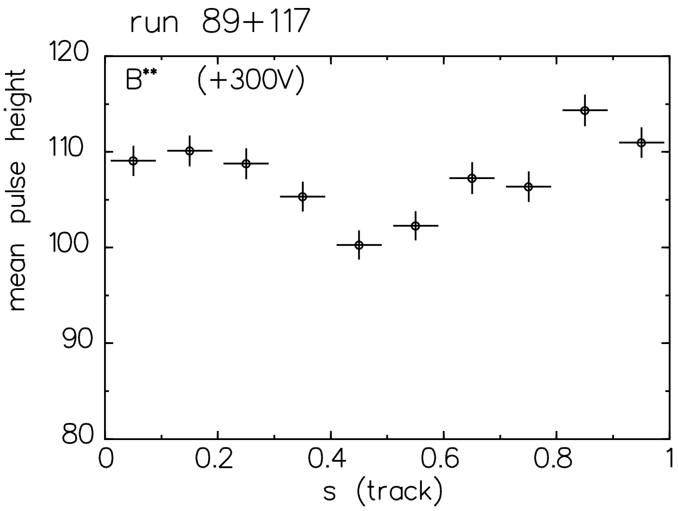

Figure 10: Average cluster charge as a function of projected track position.

6 Signal to Noise Ratio and Efficiency

An unbiased measurement of the signal to noise ratio requires that there be no threshold applied to the charge on a strip. With a track projection precision and accuracy on the order of a micron one can reliably predict which diamond detector strip should have maximum pulse height. From the distribution of the pulse height on that strip plus the greater of its two neighbors, one can obtain an unbiased distribution from which to estimate the signal to noise ratio.

Figure 11 shows the charge distribution for run 117, with the radiation-pumped 50-micron diamond operated at +300V. The mean of the distribution, 110$\pm$1 ADC counts, does not differ significantly from that obtained with the 10-ADC-count threshold. Indeed, only a few events in 9000 have summed pulse height less than 10 counts; the efficiency in this sense is nearly 100%. Given that the average noise on the strips is 3.6 ADC counts one might infer a signal-to-noise ratio of 30. Conservatively taking instead the most probable pulse height of 70 a signal-to-noise ratio of about 20 obtains. Assuming a calibration of 25.1 electrons per ADC count [1] this would imply a mean charge collection of 2750 electrons, or a collection distance of 76 μm.

In previous analyses of diamond detectors with 100-μm pitch, substantially less charge was collected when the track passed between two strips. With a pitch of 50 μm and an interstrip gap of 25 μm, the ratio of the gap to detector thickness (over 400 μm) is smaller and correspindingly one expects less “loss” of charge. Indeed, as illustrated by figure 10, roughly 10% maximum loss of charge appears in the interstrip region $0.25 < s < 0.75$.

[1] Value obtained from W. Trischuk.

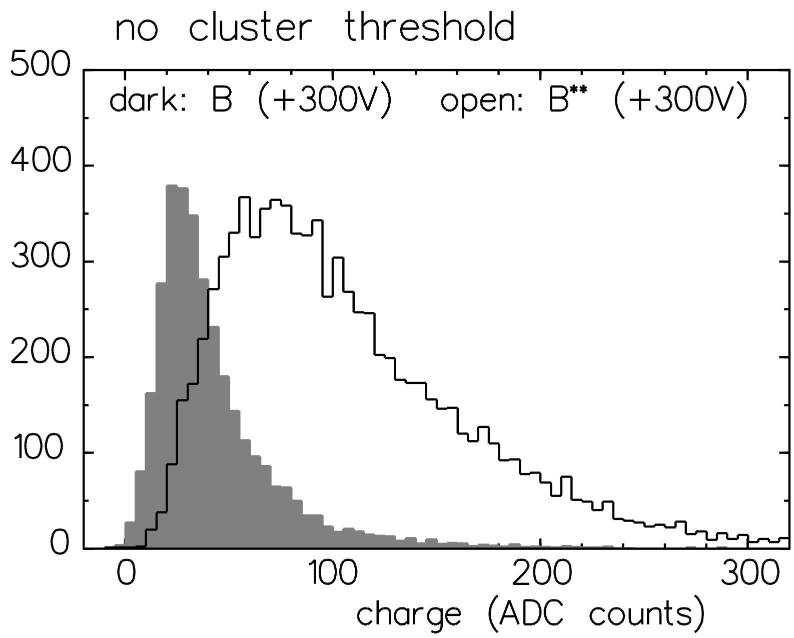

Figure 11: Unbiased pulse height distributions in the 50-micron diamond detector before and after exposure to radiation.

7 Effect of Radiation Pumping

By comparing with the data recorded before the detector was exposed to radiation one can attempt to see if the signal size increased with exposure. In run 3 the same detector was in the same location and read out by the same Sirocco. The alignment and resolution analysis proceed in an identical fashion, and the unbiased pulse height distribution appears in the shaded histogram in figure 11. The mean pulse height is 43 ± 1, a factor of 2.5 lower than that after pumping. This large factor exceeds the expected pump-up factor by at least 60%, and calls into question the reliability of both measurements.

To ascertain the source of the discrepancy one can examine the results of run 3 and other test runs in more detail. Figure 12 shows comparisons of the residuals versus eta before and after pumping. No gross problems appear, but the distribution before pumping shows diagonal streaks related to the fact that at low amplitude the choice of which side strip is used in the cluster can be affected by fluctuations. This leads to non-Gaussian tails in the residual projection shown in figure 13.

Unfortunately the other run recorded before pumping, run 4, was not analyzed. The reliability of the results in run 117, however, is bolstered by the fact that nearly identical results obtain in run 89, recorded under similar conditions. It is interesting to note that when the detector was moved in the test stand and connected to Sirocco 6 in run 146 a signal of much lower size and inverted polarity is seen. Figure 14 shows the residuals as a function of eta and the pulse height distribution. Virtually no charge sharing between strips is evident in the plot, and the residual distribution is hence that of a digital position device. The pulse height distribution has a very small mean, 38 ADC counts, but this alone does not account for the rather weird charge sharing.

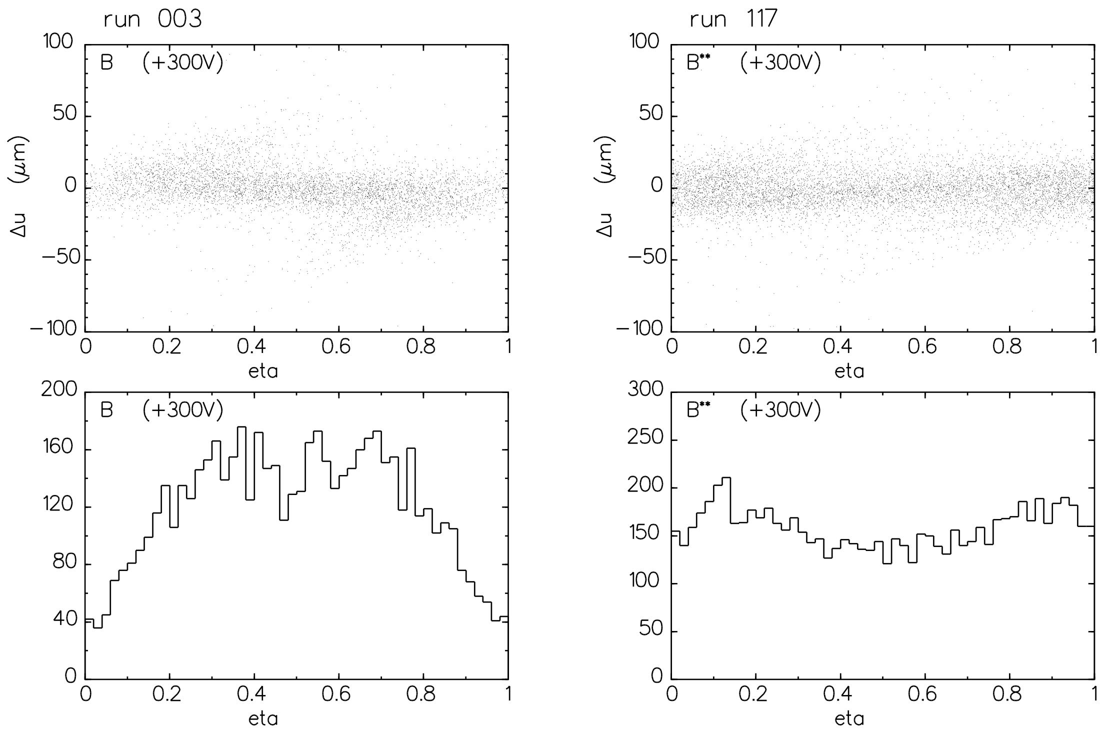

Figure 12: Track residuals in versus eta in the unpumped diamond plane (left) and after radiation pumping (right). The eta projections appear in the lower plots.

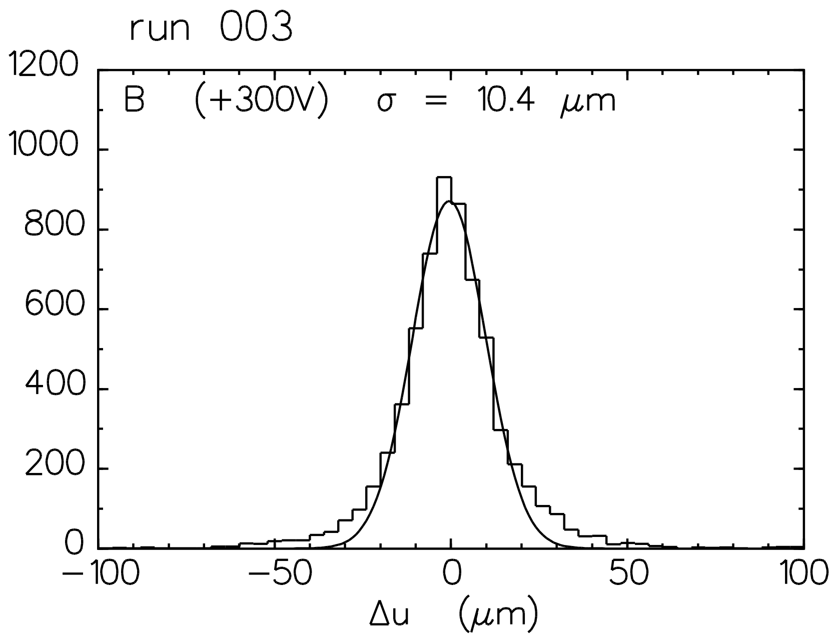

Figure 13: Spatial resolution of the 50-micron diamond detector before exposure to radiation.

8 Conclusions

The May CERN test beam data from the 50-micron detector yield several useful measurements, and raise several questions. The data indicate that

- the 50-micron-pitch detector has spatial resolution of 12.8 μm, which is only slightly better than digital resolution,
- an "eta integral deconvolution" correction to the simple weighted mean would not improve the resolution,
- the signal-to-noise ratio using the low-noise VA-2 chip lies in the range 20 (using the most probable signal) to 30 (using the mean),
- the collection distance at 300V is about 76 μm, and
- a small loss of signal appears in the 25 μm interstrip region.

The expected spatial resolution, if dominated by noise, would naively be a few microns. Why this does not obtain for the diamond eludes explanation as yet, but the data rule out several possibilities: the data exhibit no dependence of the rms of the residuals on time, pulse height, eta, or z position. One might speculate that the deposited charge spreads laterally along crystal axes while traversing the bulk, or that there is some other source of fluctuation other than electronic noise.

The measurement of the effect of radiation pumping, apparently a factor of 2.5, remains inconclusive. Though the data from the run without pumping show no serious flaws, the factor of 1.5 is too large to be explained by the effect of radiation pumping alone.

Finally, further work must be done to understand what occurred in run 146 to cause the charge sharing and pulse height to distort wildly.

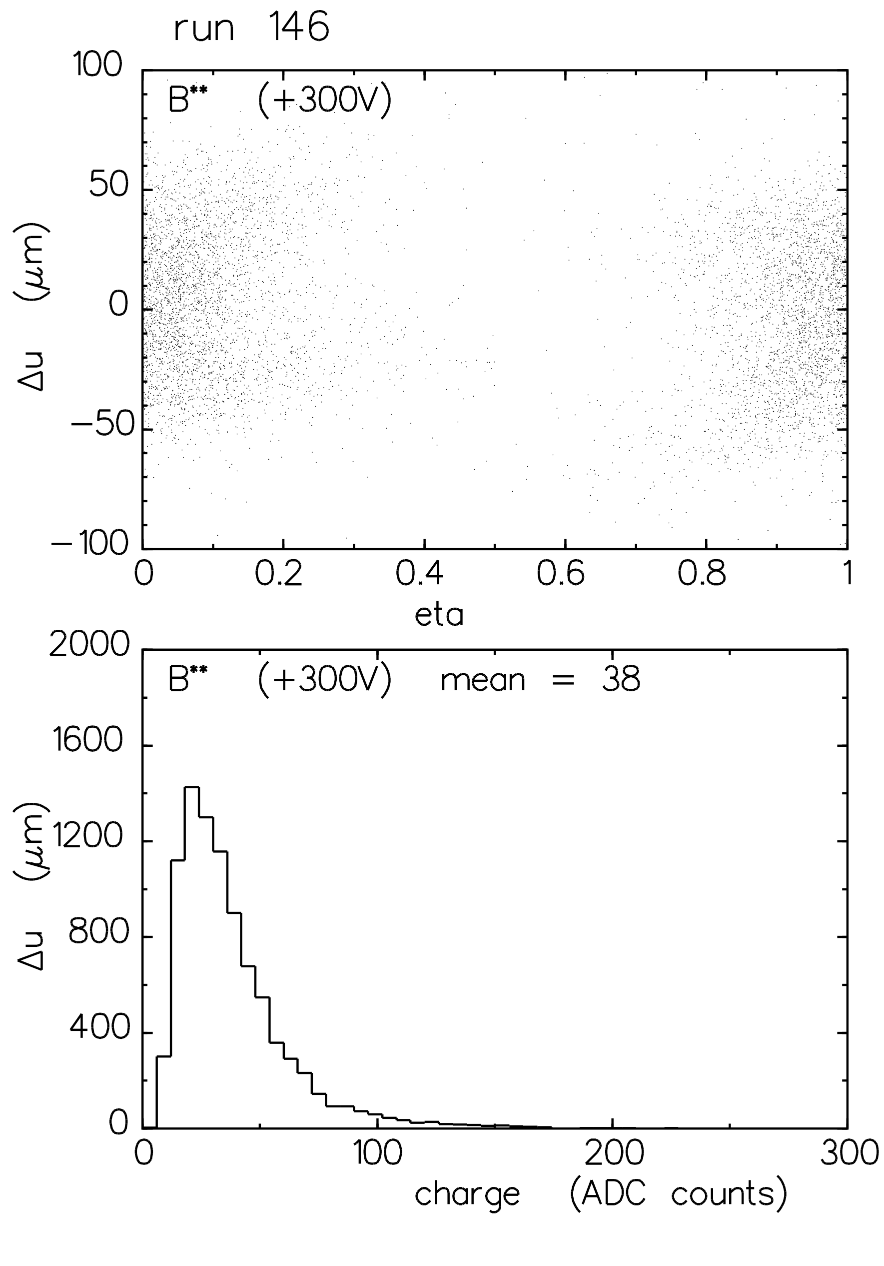

Figure 14: Residuals versus eta and pulse height distribution of the B** detector in run 146.

Acknowledgements

Many members of RD42 contributed their time and effort to make this test happen. Among them I would like to personally thank Heinz Pernegger for patiently explaining the software to me, and my colleagues Bob Stone and Steve Schnetzer for being a sounding board for my (sometimes nutty) ideas along the way.